Engineering Transactions, **71**(3): 329–349, 2023, doi: 10.24423/EngTrans.3085.20230718
Institute of Fundamental Technological Research Polish Academy of Sciences (IPPT PAN)
Université de Lorraine • Poznan University of Technology

CMM-SolMech 2022

The Dynamic Stability Problem of Composite Annular Plates with Auxetic Properties

Dorota PAWLUS

Faculty of Mechanical Engineering and Computer Science
University of Bielsko-Biala
Bielsko-Biala, Poland; e-mail: doro@ath.bielsko.pl

This paper presents the effect of the auxeticity on the behaviour of a plate subjected to the loss of stability. The plate structure is composed of three layers built of auxetic or conventional facings and a conventional core. The plate is loaded mechanically in the plane of facings with forces increasing in time. The main technique of the problem solution is based on the orthogonalisation and finite differences methods. Selected examples of plates were calculated with the use of the finite difference method. The obtained results allow observing the similarities and differences between plate models, whose structures are built of conventional layers or mixed layers: auxetic-foam-auxetic. Investigations complement the knowledge of the responses of the composite structures with auxetic properties. They show the possibility of using special plate structures whose materials are characterised by the negative value of Poisson's ratio.

Keywords: auxeticity; auxetic facings; dynamic stability; composite annular plate; three-layered structure; finite difference method; finite element method.

1. Introduction

Annular plates are one of the essential elements used in many engineering applications, for example, in the aerospace industry, mechanical and nuclear engineering, civil engineering or miniature mechanics. Among others, one of the characteristic plate structures is the classic, three-layered composite structure. Examinations of the reactions of the sandwich plates are extensive. Chen *et al.* [1] and Wang, Chen [2] can be mentioned as exemplary works, where the dynamic and stability analyses of sandwich, annular plates loaded mechanically have been performed.

Additional considerations may arise in addition to the basic requirements related to the structure, such as strength and rigidity. Among new, possible structure layer compositions, a special one can be the arrangement with the facings, whose properties are unconventional, expressed by the behaviour of

the auxetic material. The effect of the negative value of Poisson's ratio of the materials of the plate's outer layers on the dynamic response of the three-layered annular plate widens the knowledge of the behaviour of the examined plates subjected to dynamic conditions. Selected papers present the plate's reactions to special structure properties characterised by the negative values of Poisson's ratio.

The circular and annular plates with a sandwich structure composed of orthotropic facings and an auxetic core are examined in [3]. The results show the effects of the rigidity of the plate's structure, the type of support system, and the geometric dimensions. The distributions of the deflections, in-plane normal and transverse shear stresses are presented using two methods of calculation: based on the principle of the minimum total potential energy and the ABAQUS system. The static bending of a three-layered sandwich plate with an auxetic core and isotropic, homogeneous facings is presented in [4]. The multiparameter effects of the geometry, boundary system and loading are analysed. The analytically and numerically solved problem of the FGM shell and plate structures with auxetic properties is presented in [5]. The deformed shape, load distribution and edge support type are taken into consideration in [6], which presents the bending stress of the auxetic circular plate. The optimal Poisson's ratio to minimise the bending effect is examined. The axisymmetric circular plate made of isotropic auxetic and conventional material with values of Poisson's ratio within the range of -1 to 0.5 is presented in [7]. Buckling and vibration analyses are performed to evaluate the critical parameters. The compression and tension effects were analysed in paper [8] for the thin circular disks subjected to two edge loads. The eigenvalue buckling and post-buckling analyses were performed for disks made of both traditional, linear elastic and auxetic materials. The numerical results show the differences between compressed and stretched disks.

The nonlinear dynamic analysis of sandwich plates with the auxetic core subjected to the thermal environment is presented in [9]. The results show the effect of negative Poisson's ratio values on the dynamic deflections, which are smaller than for plates with a positive value of Poisson's ratio. The effect of the significant reduction of the mass and the increase of the vibration absorption of the sandwich plate structure with a negative Poisson's ratio in an auxetic honeycomb core are underlined in paper [10]. The analysed composite plate is located on the elastic foundation and loaded with a moving oscillator load composed of the spring and damper. The multiparameter problem is studied.

The complex structure of the circular plate is examined in [11]. Auxetic and porous heterogeneous plate with various thickness is located on a gradient elastic foundation. The auxeticity effect on the static behaviour of the plate is observed. The main applications of circular plates made of unconventional, auxetic material are also presented. In engineering fields, they can be found in

the power transmission systems, support tables, driven plates of a friction clutch, a disk of vehicle brakes on friction pads, and some nano-plates embedded in an elastic matrix.

In this paper, the results of the numerical examinations of the annular plates with the structure composed of auxetic-foam-auxetic materials are presented aimed at enriching the analyses of this new type of composite plates. The examinations of the annular plates with the structure of the three-layered composite with conventional and auxetic properties are conducted with the use of two calculation techniques: the analytical technique using the finite difference method and the numerical technique using finite elements. The plates are subjected to linear loads quickly increasing in time. Two different load cases are analysed: plates radially compressed on the outer edge and plates radially stretched on the inner edge. The case of "buckling at the stretching", which is rarely examined, significantly complements the evaluation of plate behaviour with specific auxetic properties. The numerous calculation results create the image of dynamic responses of the examined structures on the effect of the various positive and negative values of Poisson's ratio of the facing material of the plates, whose reactions to the auxeticity phenomenon are different.

2. Problem formulation

A composite, three-layered annular plate is the object of the analysis. The plate structure is composed of thin facings made of auxetic or conventional materials and a thicker conventional foam core. Figure 1 shows the loading scheme of the plate. Both plate edges are slideably clamped. The plate is loaded

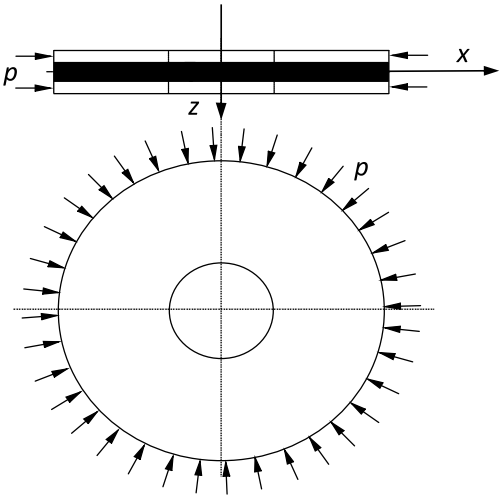

Fig. 1. The scheme of the plate.

in the plane of facings with the forces quickly and linearly increasing in time according to Eq. (2.1):

$$p = st, \tag{2.1}$$

where p – loading stress, s – the rate of the loading growth, t – time.

Such loading can be the reason for the loss of plate stability. To determine the parameters of the critical plate state, such as time, load and deflection, the criterion presented by Volmir [12] is adopted. According to this criterion, the loss of stability occurs at the moment when the point of the plate with the maximum deflection reaches the first maximum value of the velocity of deflection. The black dots in Figs. 3, 4, and 7 represent the moment of the loss of plate stability, which is specified according to the presented criterion.

Two models of plate loading are examined: a plate radially compressed or radially stretched. The case of the plate radially stretched, named "buckling at the stretching", is not a typical buckling problem. It exists for the annular plate specifically loaded on the inner edge with the forces directed to the middle of the hole. The evaluation of the effect of the positive and negative value of Poisson's ratio on the plate's dynamic reaction is conducted for plates whose layers are both compressed and stretched. It makes the examined problem more complete. The range of the accepted values of Poisson's ratio is large from negative value $\nu = -0.9$ to positive $\nu = 0.3$. Selected values of Poisson's ratio ν were taken into numerical calculations.

3. Solution procedure

The presented problem is solved analytically and numerically using the approximation methods: the analytical and numerical method with the usage of the orthogonalisation and finite difference methods (FDM), and the second method is the numerical one based on the finite element method (FEM). Two FDM and FEM plate models allow observing axisymmetric and asymmetric buckling forms of plate deformation for conventional and auxetic structures. The solution procedure based on the finite difference method refers to the technique presented in the following works [13–15].

The analyses of results obtained for two FDM and FEM plate models confirm the observed behaviours of auxetic plates and enable the comparison of both numerical models. Additionally, results mutually complement and enrich the recognition of the problem.

The second solution is the FEM. Using the ABAQUS system, selected examples of plates are examined.

3.1. FDM

The solution procedure using the FDM is based on several fundamental steps. They are as follows: the system of the dynamic equilibrium equations of each plate layer, the relations describing the transversal deformation of the plate's three-layered structure using the classical broken line hypothesis, which is based on the participation of plate layers in carrying the plate load: the facings are loaded with normal but the core with shear stresses [16], the equations of the linear physical relations, and the use of the assumed stress function to express the resultant membrane forces.

After the calculations and transformations, the basic equation is established, which describes the deflections of the plate loaded dynamically:

$$
\begin{aligned}
(3.1)\quad & k_1 w_{d'rrrr} + \frac{2k_1}{r} w_{d'rrr} - \frac{k_1}{r^2} w_{d'rr} + \frac{k_1}{r^3} w_{d'r} \\
& + \frac{k_1}{r^4} w_{d'\theta\theta\theta\theta} + \frac{2\,(k_1+k_2)}{r^4} w_{d'\theta\theta} + \frac{2k_2}{r^2} w_{d'rr\theta\theta} - \frac{2k_2}{r^3} w_{d'r\theta\theta} \\
& - G_2 \frac{H'}{h_2} \frac{1}{r} \left(\gamma_{\prime\theta} + \delta + r\delta_{\prime r} + H' \frac{1}{r} w_{d'\theta\theta} + H' w_{d'r} + H' r w_{d'rr} \right) \\
& = \frac{2h'}{r} \left(\frac{2}{r^2} \Phi_{\prime\theta} w_{\prime r\theta} - \frac{2}{r} \Phi_{\prime r\theta} w_{\prime r\theta} + \frac{2}{r^2} w_{\prime\theta} \Phi_{\prime r\theta} - \frac{2}{r^3} w_{\prime\theta} \Phi_{\prime\theta} + w_{\prime r} \Phi_{\prime rr} \right. \\
& \left. + \Phi_{\prime r} w_{\prime rr} \frac{1}{r} \Phi_{\prime\theta\theta} w_{\prime rr} + \frac{1}{r} \Phi_{\prime rr} w_{\prime\theta\theta} \right) - M w_{d'tt},
\end{aligned}
$$

where w_d – the additional plate deflection, r – plate radius, $k_1 = 2D$, $k_2 = 4D_{r\theta} + \nu k_1$, $D = \frac{Eh^3}{12(1-\nu^2)}$, $D_{r\theta} = \frac{Gh^3}{12}$ – rigidities of the plate facings, E, ν – Young's modulus and Poisson's ratio of the auxetic or conventional facing material, respectively; h – the total plate thickness, δ, γ – differences of radial and circumferential displacements of the points in the middle surfaces of the facings $\delta = u_3 - u_1$, $\gamma = v_3 - v_1$, $H' = h' + h_2$, Φ – the stress function, w – the plate total deflection, $M = 2h'\mu + h_2$; μ, μ_2 – facing and core mass density, h' – the facing thickness, and h_2 – the core thickness.

Both plate edges are slideably clamped. The boundary conditions are as follows:

$$
\begin{aligned}
(3.2)\quad & w|_{r=r_i(r_o)} = 0, \qquad w_{\prime r}|_{r=r_i(r_o)} = 0, \\
& \delta = \gamma|_{r=r_i(r_o)} = 0, \qquad \delta_{\prime r}|_{r=r_i(r_o)} = 0.
\end{aligned}
$$

The initial conditions for the additional plate deflection are presented by the relations:

$$
(3.3)\qquad w_d|_{t=0} = 0, \qquad w_{d,t}|_{t=0} = 0.
$$

The following conditions are connected with the mechanical loading of the plate:

$$\sigma_r|_{r=r_i} = -p\,(t)\,d_1, \qquad \sigma_r|_{r=r_o} = -p\,(t)\,d_2, \tag{3.4}$$
$$\tau_{r\theta}|_{r=r_i(r_o)} = 0,$$

where σ_r – radial stress, $\tau_{r\theta}$ – shear stress, d_1, d_2 – quantities, equal to 0 or 1, determining the loading of the inner or/and outer plate perimeter, and r_i, r_o – the inner and outer plate radius, respectively.

The preliminary plate shape is not absolutely flat. The plate has preliminary deflections. The form of plate imperfection, expressed by the preliminary deflection ζ_o ($\zeta_o = w_o/h$), is expressed by the accepted relation [17]:

$$\zeta_o\,(\rho,\theta) = \xi_1\,(\rho)\,\eta\,(\rho) + \xi_2(\rho)\eta\,(\rho)\cos\,(m\theta), \tag{3.5}$$

where w_o – plate initial deflection, m – number of initial circumferential waves, ξ_1, ξ_2 – calibrating numbers, $\eta\,(\rho)$ – function: $\eta\,(\rho) = \rho_4 + A_1\rho_2 + A_2\rho_2 \ln\rho + A_3 \ln\rho + A_4$, A_i – quantities fulfilling the conditions of clamped edges, and $\rho = \frac{r}{r_o}$ – the dimensionless plate radius.

The solution procedure is based on some shape functions connected with the plate's additional deflection, radial and circumferential displacements and accepted stress function. The equations are as follows:

- for the additional plate deflection ζ_1 [17]:

$$\zeta_1\,(\rho,\theta,t) = X_1(\rho,t)\cos\,(m\theta), \tag{3.6}$$

- for the differences of the radial and circumferential displacements $\overline{\delta}$, $\overline{\gamma}$ [14]:

$$\overline{\delta}\,(\rho,\theta,t) = \overline{\delta}\,(\rho,t)\cos\,(m\theta), \tag{3.7}$$
$$\overline{\gamma}\,(\rho,\theta,t) = \overline{\gamma}\,(\rho,t)\sin\,(m\theta),$$

- for the accepted stress function F [17]:

$$F(\rho,\theta,t) = F_a(\rho,t) + F_b(\rho,t)\cos\,(m\theta) + F_c(\rho,t)\cos\,(2m\theta), \tag{3.8}$$

where $\zeta_1 = \frac{w_d}{h}$, $F = \frac{\Phi}{Eh^2}$, $\overline{\delta} = \frac{\delta}{h}$, $\overline{\gamma} = \frac{\gamma}{h}$, and m – the number of circumferential waves, which is compatible with the initial number of waves (see Eq. (3.5)).

The following part of the solution procedure is based on the use of the approximation methods. For the elimination of the angular variable θ, the orthogonalisation method was used. The derivatives with respect to ρ were approximated by the central differences in the discrete points of the finite difference method.

The main system of the differential equations for the analysed plate has the following form:

$$\mathbf{PU} + \mathbf{Q} = \ddot{\mathbf{U}}_K, \tag{3.9}$$

$$\mathbf{M}_Y\mathbf{Y} = \mathbf{Q}_Y, \tag{3.10}$$

$$\mathbf{M}_V\mathbf{V} = \mathbf{Q}_V, \tag{3.11}$$

$$\mathbf{M}_Z\mathbf{Z} = \mathbf{Q}_Z, \tag{3.12}$$

$$\mathbf{M}_{GG}\mathbf{G} + \mathbf{M}_{GU}\mathbf{U} + \mathbf{M}_{GD}\mathbf{D} = \mathbf{0}, \tag{3.13}$$

where $\mathbf{U}$, $\mathbf{Y}$, $\mathbf{V}$, $\mathbf{Z}$ – vectors, whose elements consist of the additional deflections and components of the stress function, respectively, $\ddot{\mathbf{U}}_K$ – a vector, whose elements are expressed by the products of the derivative of the additional deflection with respect to time t and number K, equal to $K = K7^2 \cdot \frac{h'}{h} \cdot r_o h_2 M$, $\mathbf{Q}$, $\mathbf{Q}_V$, $\mathbf{Q}_Y$, $\mathbf{Q}_z$, $\mathbf{D}$, $\mathbf{G}$ – vectors, whose elements consist of the plate's material parameters, geometrical dimensions, initial and additional deflections, number m, dimension radius ρ and displacement differences δ, γ, and $\mathbf{M}_Y$, $\mathbf{M}_V$, $\mathbf{M}_Z$, $\mathbf{M}_D$, $\mathbf{M}_G$, $\mathbf{M}_U$, $\mathbf{M}_{GG}$, $\mathbf{M}_{GD}$, $\mathbf{P}$, $\mathbf{M}_{GU}$ – matrices, whose elements consist of the plate's material parameters, geometrical dimensions, number m, FDM parameter b (b – the interval in the FDM) and dimension radius ρ.

The numerical calculations are conducted using Runge-Kutta's integration method for the initial state of the plate. The time was expressed by dimensionless time t^* connected with real time t (see Eq. (2.1)) by the relation: $t^* = t \cdot K7$, where $K7$ is the number expressing the rate of mechanical loading growth.

3.2. FEM

Calculation using the finite element method is conducted in the ABAQUS system at the Academic Computer Centre CYFRONET-CRACOW (KBN/SGI_ORIGIN_2000/PLodzka/030/1999). The plate structure is built of shell and solid elements. The facings are modelled with 3D 9-node shell elements, but the core layer is modelled with 3D 27-node solid elements. The surface contact interaction with the TIE option was assumed to connect the surfaces of the facings and the core meshes. Dynamic analyses were conducted by applying the dynamic module of the ABAQUS programme [18].

Obtained results complement the calculation results of the FDM plate model, for example, through the maps of critical deflections. Presented two FDM and FEM plate models are compared. Some comments can be useful in the modelling of plates and similar structures. The character of observed plate behaviours is confirmed.

4. Exemplary results

Exemplary results are calculated for the annular plate with the following geometrical parameters: inner radius $r_i = 0.2$ m, outer radius $r_o = 0.5$ m, facing thickness $h' = 1$ mm, and core thickness $h_2 = 5$ mm. The plate structure is composed of outer layers and a core made of isotropic materials with conventional or auxetic properties, with the value of Young's modulus equal to $E = 1550$ MPa, the value of Poisson's ratio $\nu = 0.3,\ 0,\ -0.3,\ -0.6,\ -0.9$, mass density $\mu = 1500$ kg/m^3 and polyurethane foam with the value of Young's modulus equal to $E_2 = 13$ MPa, the value of Kirchhoff's modulus $G_2 = 5$ MPa, the value of Poisson's ratio $\nu_2 = 0.3$ and mass density $\mu_2 = 64$ kg/m^3. The value of Young's modulus facings equal to $E = 1550$ MPa is fixed. Treating both conventional and auxetic facings material as isotropic for the fixed value of Young's modulus and accepted variable values of Poisson's ratio, the values of Kirchhoff's modulus, which are related to them, change. The value of Young's modulus was adopted to be equal to 1550 MPa from [19], where it was obtained based on the simulation process for the laminated periodic composite material with auxetic properties.

Two models of plate loading are considered. A plate radially compressed on the outer edge (see Fig. 2a) and a plate radially stretched on the inner edge (see Fig. 2b). The plate is loaded mechanically with the stress linearly increasing in time (see Eq. (2.1)). The value of the rate of loading growth is equal to $s = 100$ MPa/s.

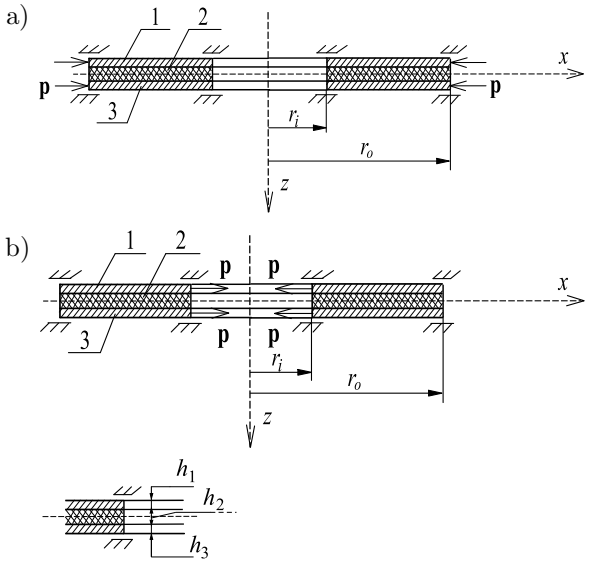

Fig. 2. Scheme of the plate (1, 3 – facings, 2 – core): a) radially compressed on the outer edge, b) radially stretched on the inner edge with the thickness dimensions of layers.

4.1. Convergence analysis for the FDM plate model

Tables 1–3 present the values of the critical dynamic loads p_{crdyn} calculated for the different plate modes and numbers of discrete points N used in the FDM. The convergence evaluation is performed for the auxetic plates radially compressed and stretched with the values of Poisson's ratio equal to $\nu = -0.3$, -0.9, and -0.6, respectively. The selected numbers of discrete points are equal to $N = 11$, 14, 17, 21, 26.

Table 1. The values of the dynamic, critical stress differences p_{crdyn} depending on the number N of discrete points for the FDM auxetic plate model radially compressed on the outer edge with the value of Poisson's ratio $\nu = -0.3$ loaded.

m	p_{crdyn} [MPa]				
	$N = 11$	$N = 14$	$N = 17$	$N = 21$	$N = 26$
0	8.55	8.20	8.00	7.85	7.75
1	8.05	7.75	7.60	7.45	7.35
2	6.65	6.40	6.30	6.20	6.20
3	5.35	5.25	5.15	5.10	5.10
4	4.70	4.60	4.60	4.55	4.50
5	**4.45**	**4.40**	**4.40**	**4.35**	**4.35**
6	4.50	4.45	4.45	4.40	4.40
7	4.65	4.65	4.60	4.60	4.60
8	4.95	4.90	4.90	4.90	4.90

Table 2. The values of the dynamic, critical stress differences p_{crdyn} depending on the number N of discrete points for the FDM auxetic plate model radially compressed on the outer edge with the value of Poisson's ratio $\nu = -0.9$.

m	p_{crdyn} [MPa]				
	$N = 11$	$N = 14$	$N = 17$	$N = 21$	$N = 26$
0	16.05	15.90	15.80	15.75	15.70
1	15.30	15.15	15.10	15.05	15.05
2	12.80	12.70	12.70	12.65	12.65
3	10.65	10.60	10.60	10.60	10.60
4	9.55	9.55	9.55	9.55	9.55
5	9.10	9.10	9.10	9.15	9.15
6	**9.05**	**9.05**	**9.05**	**9.05**	**9.10**
7	9.15	9.15	9.20	9.20	9.20
8	9.35	9.40	9.40	9.40	9.40
9	9.65	9.65	9.65	9.70	9.65
10	10.40	10.35	10.35	10.30	10.30

Table 3. The values of the dynamic, critical stress differences p_{crdyn} depending on the number N of discrete points for the FDM auxetic plate model radially stretched on the inner edge with the value of Poisson's ratio $\nu = -0.6$.

m	p_{crdyn} [MPa]				
	$N = 11$	$N = 14$	$N = 17$	$N = 21$	$N = 26$
5	19.55	19.50	19.45	19.40	19.40
6	17.50	17.45	17.45	17.45	17.45
7	**17.10**	**17.10**	**17.10**	**17.10**	**17.10**
8	17.70	17.50	17.55	17.55	17.55
9	18.10	18.05	18.20	18.15	18.20

Shown above arrays of numbers p_{crdyn} enable formulating the following observations:

- the number $N = 14$ fulfils the appropriate accuracy, which is expressed by a technical error of up to 5%. The number $N = 14$ was used in numerical calculations,
- the minimal values of critical dynamic loads p_{crdyn} are for the wavy forms of plate buckling,
- the values of p_{crdyn} for the axisymmetric ($m = 0$) plate mode are about two times larger than for the asymmetric mode, which corresponds to the minimal value of p_{crdyn}. It confirms the importance of the generalised way of the problem solution, which includes the asymmetric forms of plate buckling,
- the differences between the values p_{crdyn} for plates with higher modes are much smaller than between the lower mode numbers,
- for the stretched plates with circumferential waves, the fluctuations of values p_{crdyn} versus the numbers N are small. The translation to the higher mode ($m = 7$) for the minimal value of the critical dynamic load p_{crdyn} is observed.

4.2. FDM plate model radially compressed on the outer edge

Figure 3 presents the time histories of deflections of auxetic plates radially compressed on the outer edge.

Two cases of auxetic material of plate facings are analysed: with the value of Poisson's ratio equal to $\nu = -0.3$ and the extreme value of Poisson's ratio equal to $\nu = -0.9$. The minimal value of the calculated critical dynamic load p_{crdyn} is equal to $p_{crdyn} = 4.4$ MPa for plate mode $m = 5$ with auxetic facings $\nu = -0.3$

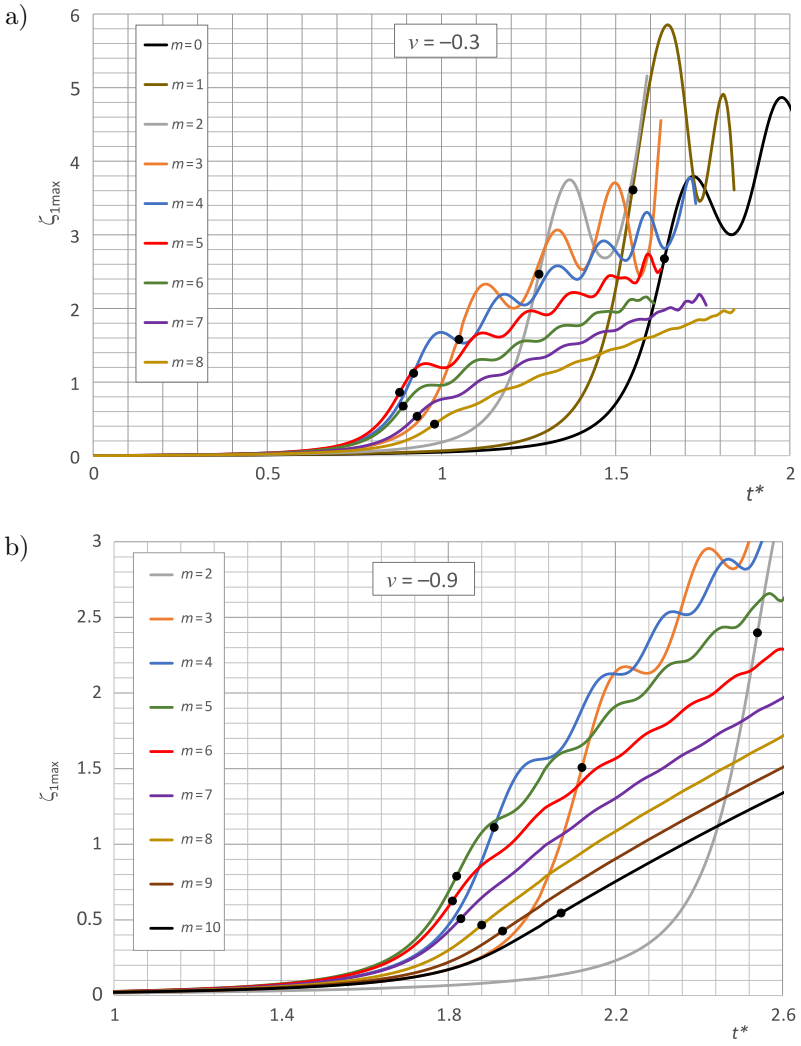

FIG. 3. Time histories of deflections for the FDM plate model radially compressed on the outer edge with auxetic facings with the value of Poisson's ratio: a) $\nu = -0.3$, b) $\nu = -0.9$.

and $p_{crdyn} = 9.05$ MPa for plate mode $m = 6$ with auxetic facings $\nu = -0.9$. In the overcritical region of the plate work, the vibrations are initiated by the increasing load.

Figure 4 shows the groups of dynamic results for modes $m = 4, 5, 6$ of plates with conventional and auxetic facings. Results depend on the values of Poisson's ratio ν. The minimal values of critical dynamic load p_{crdyn} are for plate facings with $\nu = 0$ and the examined cases of conventional ($\nu = 0.3$) and auxetic ($\nu = -0.3$) plate structures.

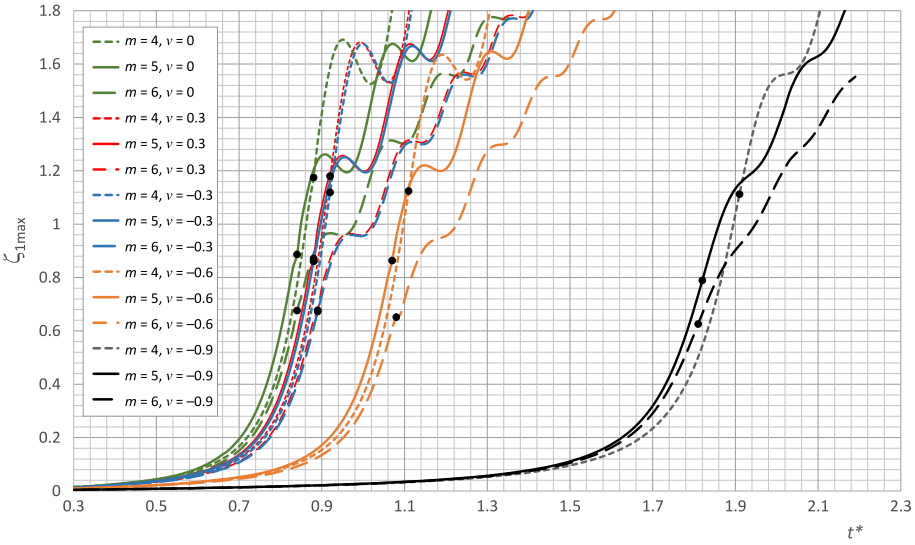

FIG. 4. Time histories of deflection for the FDM plate model radially compressed on the outer edge with auxetic and conventional facings for various values of Poisson's ratio.

Table 4, in detail, shows the values of critical, dynamic loads p_{crdyn}.

Table 4. Critical dynamic loads p_{crdyn} for the FDM plate model radially compressed on the outer edge with auxetic and conventional facings for various values of Poisson's ratio.

m	p_{crdyn} [MPa]				
	$\nu = 0$	$\nu = 0.3$	$\nu = -0.3$	$\nu = -0.6$	$\nu = -0.9$
4	4.4	4.6	4.6	5.55	9.55
5	4.2	4.4	4.4	5.35	9.1
6	4.2	4.45	4.45	5.4	9.05

Summarising, it can be observed that

- the form of the loss of plate dynamic stability is asymmetrical with $m = 5$ or $m = 6$ circumferential waves,
- the agreement of plate behaviours between plates with auxetic ($\nu = -0.3$) and conventional ($\nu = 0.3$) structures exists,
- much higher values of critical dynamic load p_{crdyn} are observed for plates with a high absolute value of Poisson's ratio of auxetic facings.

4.3. FEM plate model radially compressed on the outer edge

Time histories of deflections and velocity of deflections for the FEM plate models radially compressed on the outer edge with various values of Poisson's

ratio are shown in Fig. 5. Four cases are presented for auxetic facings with the values of Poisson's ratio equal to $\nu = 0, -0.3, -0.6, -0.9$. Selected values of

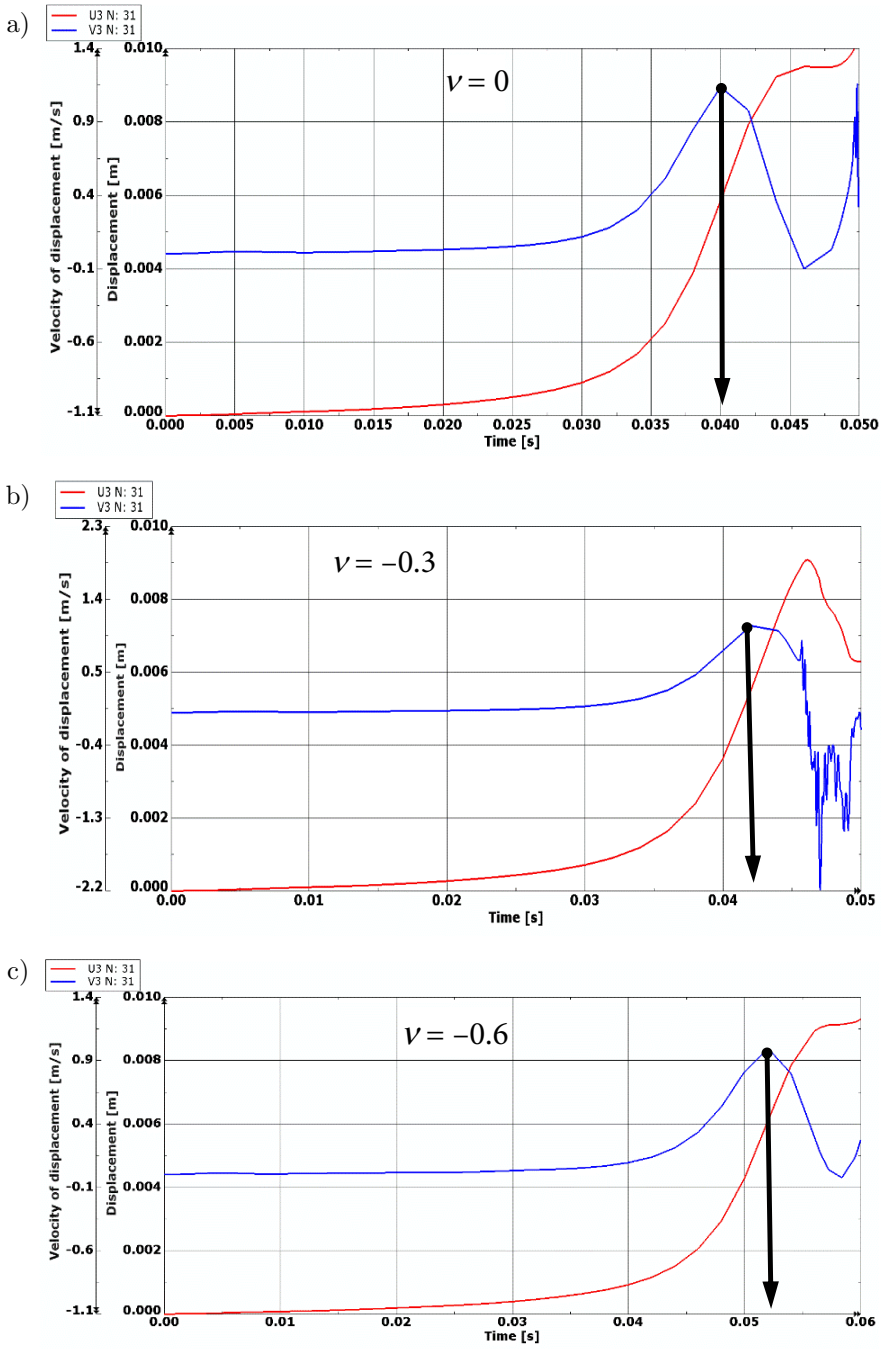

[FIG. 5abc].

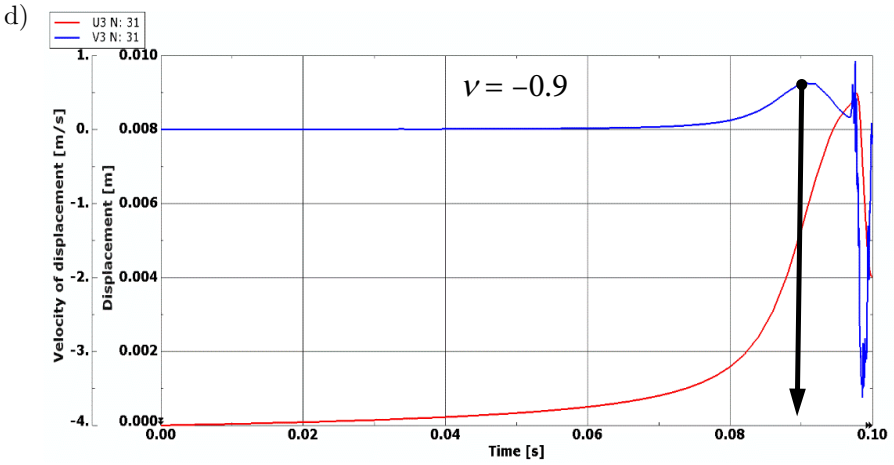

FIG. 5. Time histories of deflections and velocity of deflections for FEM plate models radially compressed on the outer edge with various values of Poisson's ratio:
a) $\nu = 0$, b) $\nu = -0.3$, c) $\nu = -0.6$, d) $\nu = -0.9$.

Poisson's ratio agree with values adopted in the FDM analysis in order to present the comparison of two FDM and FEM plate models and confirm observed plate behaviours.

Marked by the down arrow, the point of the velocity curve indicates the moment of the loss of plate stability assigned by the adopted criterion. With the increase of the absolute value of Poisson's ratio, the time to the loss of plate stability is prolonged. The detailed values of p_{crdyn} are presented in Table 5. Table 5 shows the comparison between the two analysed plate models FEM and FDM. The results are comparable. The smaller values are for the FEM plate model.

Table 5. Critical dynamic loads p_{crdyn} for the FDM and FEM plate models radially compressed on the outer edge with auxetic and conventional facings for various values of Poisson's ratio.

	p_{crdyn} [MPa]				
	$\nu = 0$	$\nu = 0.3$	$\nu = -0.3$	$\nu = -0.6$	$\nu = -0.9$
m	5				6
FDM	4.2	4.4	4.4	5.35	9.05
m	5				
FEM	4.0	4.2	4.2	5.2	9.0

The additional calculation results of modes $m = 4$ and $m = 6$ are presented in Fig. 6 for the auxetic FEM plate model with the value $\nu = -0.9$. The loss of

dynamic stability of the plate with $m = 4$ or $m = 6$ is for the higher value of time t ($t > 0.09$ s) than for the plate with $m = 5$, whose critical dynamic load p_{crdyn} is the smallest ($t = 0.09$ s, see Fig. 5d). The maps of deflections show the forms of plate buckling and the values of deflections, whose value decreases with the increase of number m. The overcritical vibrations are observed for lower plate mode $m = 4$.

Summarising the comparative analysis of two FDM and FEM plate models, the following conclusions can be formulated:

- the minimal value of the critical dynamic load p_{crdyn} is for the asymmetric plate mode ($m = 5$, $m = 6$),

a)

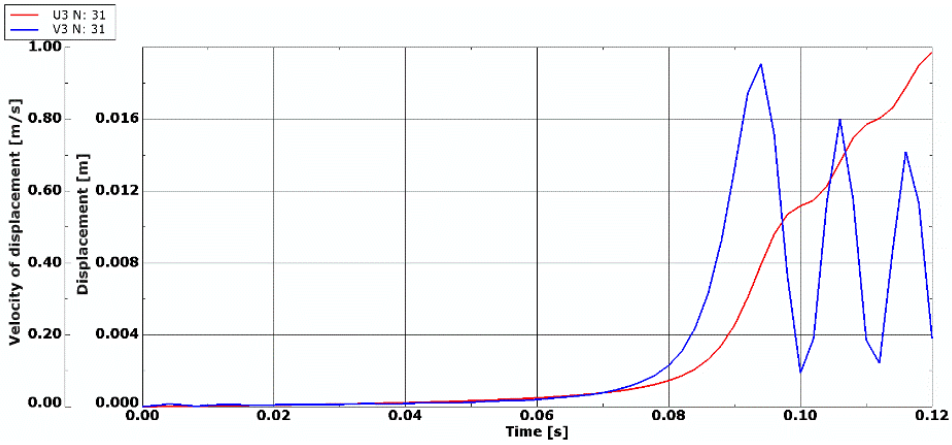

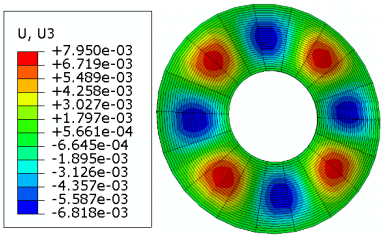

b)

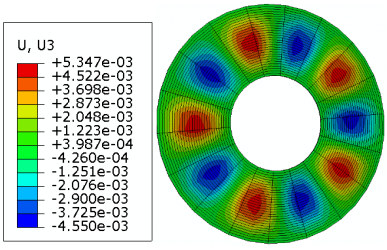

[FIG. 6ab].

c)

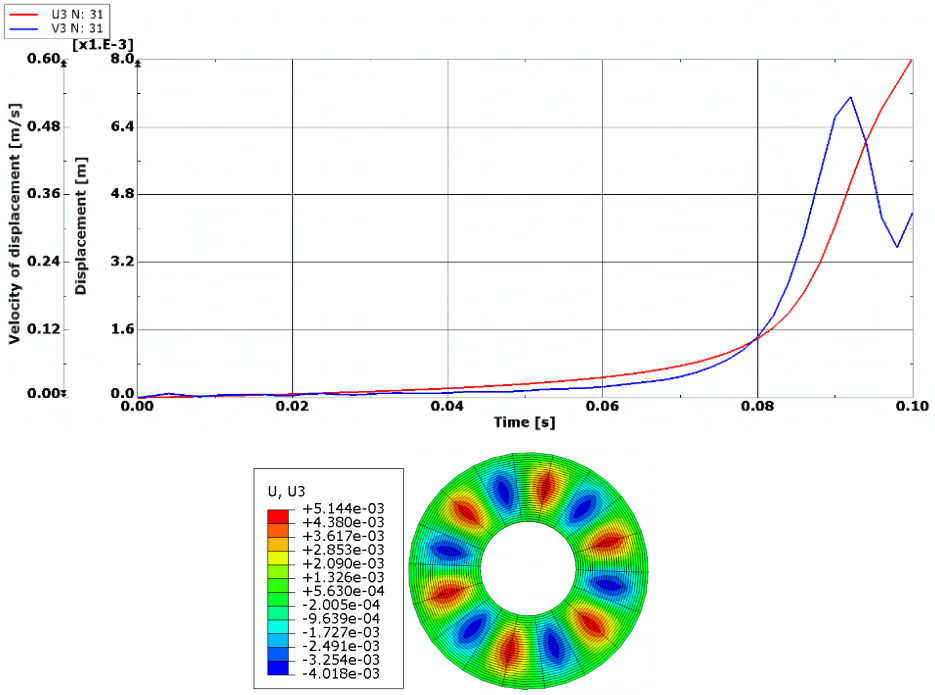

FIG. 6. Results of FEM plate models radially compressed on the outer edge with value of Poisson's ratio $\nu = -0.9$: a) time histories of deflections and velocity of deflections with map of deflections for $m = 4$ mode, b) map of critical deflections for $m = 5$ mode, c) time histories of deflections and velocity of deflections with map of deflections for $m = 6$ mode.

- the increase of the absolute value of Poisson's ratio prolongs the critical time to the loss of plate stability and increases the value of the critical dynamic load p_{crdyn},
- the vibrations initiated in the overcritical region of plate work decrease for plates with a higher absolute value of Poisson's ratio,
- there is a good comparison between the results obtained for the FDM and FEM plate models.

4.4. FDM plate model radially stretched on the inner edge

Figure 7 presents the results of the calculations of the annular FDM plate model radially stretched on the inner edge. Results depend on the values of Poisson's ratio ν. There are groups of the results for the plate modes $m = 6$, 7, 8 for plate structures with conventional and auxetic facings. For the plate with the negative value of auxetic facings equal to $\nu = -0.9$, six deflection curves are presented for $m = 6$–11.

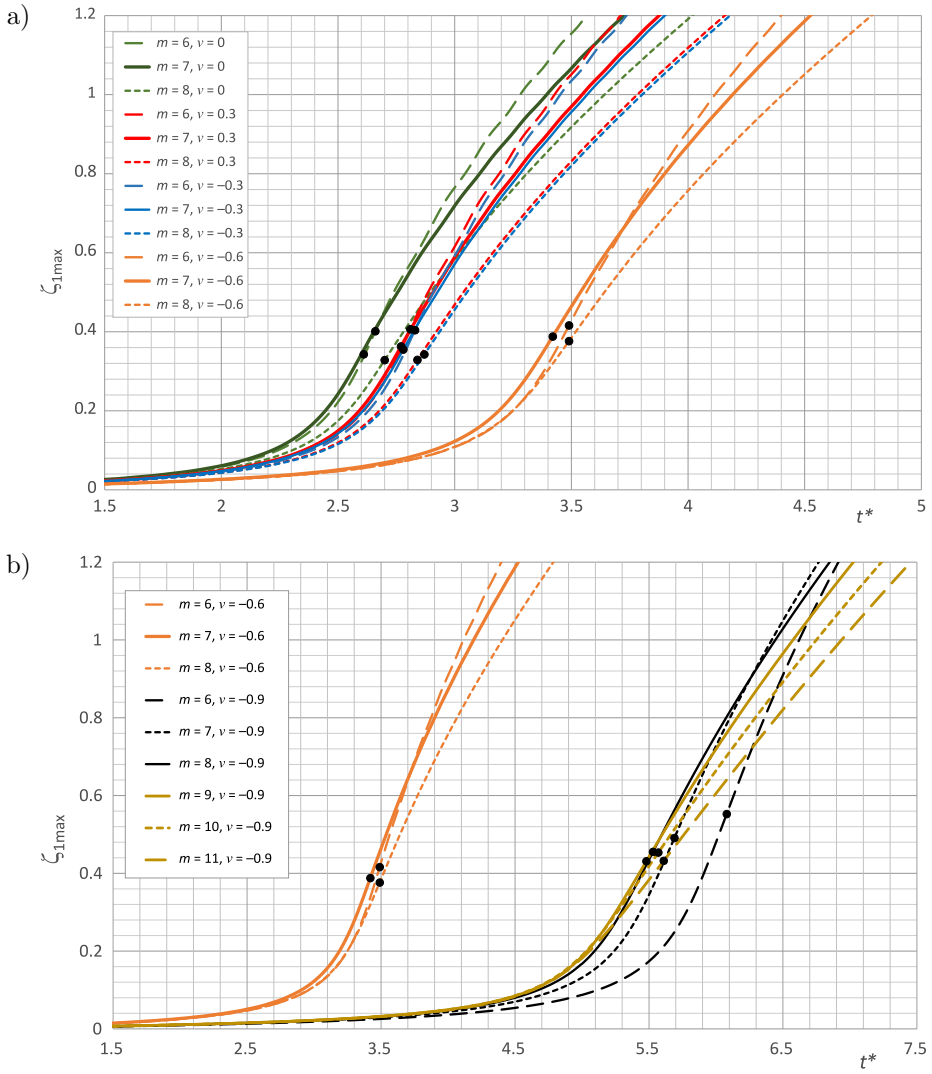

FIG. 7. Time histories of deflection for the FDM plate model radially stretched on the inner edge with auxetic facings for the following values of Poisson's ratio: a) $\nu = 0$, $\nu = 0.3$, $\nu = -0.3$, $\nu = -0.6$, b) $\nu = -0.6$, $\nu = -0.9$.

The results confirm the observations presented for the plate mode compressed on the outer edge. The minimal value of the critical load p_{crdyn} is for the plate structure with $\nu = 0$. For the higher value of Poisson's ratio, the values of p_{crdyn} increase. The asymmetric form of buckling with the seven circumferential buckling waves occurs for all of the analysed cases except for the auxetic plate with $\nu = -0.9$. For this example, the critical buckling form is expressed by the plate mode $m = 9$.

The values are presented in detail in Table 6.

Table 6. Critical dynamic loads for the FDM plate model radially stretched on the inner edge with auxetic and conventional facings for various values of Poisson's ratio.

m	p_{crdyn} [MPa]				
	$\nu = 0$	$\nu = 0.3$	$\nu = -0.3$	$\nu = -0.6$	$\nu = -0.9$
4	19.95	21.00	21.20	26.15	46.90
5	14.80	15.60	15.75	19.50	34.65
6	13.30	14.05	14.15	17.45	30.40
7	13.05	13.85	13.90	17.10	28.45
8	13.50	14.20	14.35	17.45	27.65
9	14.55	15.15	15.10	18.20	27.40
10	15.40	15.95	15.90	19.25	27.85
11	15.95	16.65	17.10	20.45	28.05

To summarise, one can notice that

- the form of the loss of plate dynamic stability is asymmetrical,
- for the value of $\nu = -0.9$, the buckling mode moves to $m = 9$,
- for higher values of Poisson's ratio for auxetic facings, the critical dynamic load p_{crdyn} is higher.

4.5. FEM plate model radially stretched on the inner edge

The results obtained for the auxetic FEM plate model with $\nu = -0.6$ are shown in Figs. 8 and 9. Figure 8 shows the time histories of deflections and velocity of deflections of the plate model radially stretched on the inner edge.

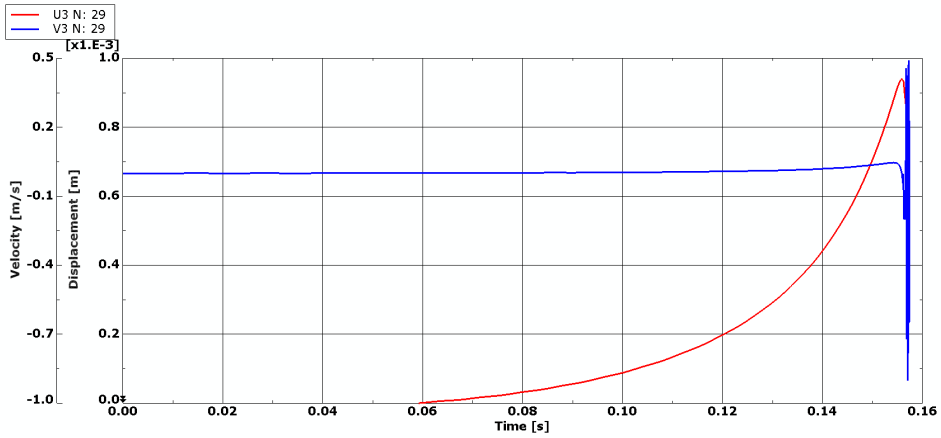

FIG. 8. Time histories of deflections and velocity of deflections for the FEM plate model radially stretched on the inner edge with value $\nu = -0.6$ of Poisson's ratio and mode $m = 7$.

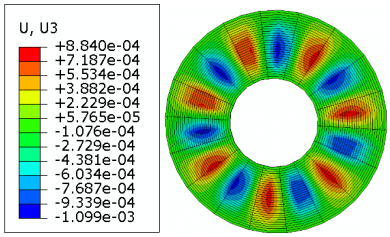

FIG. 9. Map of critical deflections of the FEM plate model radially stretched on the inner edge with the value $\nu = -0.6$ of Poisson's ratio and mode $m = 7$.

The case of the plate mode with $m = 7$ of buckling waves is presented. The critical deflection map is shown in Fig. 9. The other examined FEM plate modes $m = 6$ and $m = 8$ confirm the plate reaction observed for $m = 7$. Values of p_{crdyn} are similar and equal to $p_{crdyn} = 15.7$ MPa for m $= 6$, $p_{crdyn} = 15.4$ MPa for $m = 7$, and $p_{crdyn} = 15.4$ MPa for $m = 8$.

Comparing the results obtained for two FDM and FEM plate models radially stretched on the inner edge with the value of Poisson's ratio equal to $\nu = -0.6$ for the auxetic facings, the following conclusions can be formulated:

- the critical dynamic load p_{crdyn} calculated for the FEM plate model is smaller than that calculated for the FDM plate model (see Tables 5 and 6),
- there are no great differences in values of p_{crdyn} between plate modes $m = 6$,7,8, which designate the critical buckling form of the plate at the moment of the loss of dynamic stability,
- the plate subjected to the "buckling at the stretching" requires higher values of a load than the plate under the compression on the outer edge. It shows significant differences between the actions of traditional compressive loads and stretched loads.

5. CONCLUSIONS

The presented problem shows the responses of three-layered annular plates laterally mechanically loaded on the negative values of Poisson's ratio of the facings layers. Numerous numerical calculations enabled creating a dynamic image of the auxeticity effect. They complete the results shown for the same plate object but subjected to static analysis presented in [20]. The main aim of the undertaken investigations has been realised. The comparisons of the plate's buckling behaviours have been conducted between three-layered structures: auxetic-foam-auxetic and between the auxetic and conventional materials of plate facings. The observations are composed of calculation results of both FDM and FEM plate models. The results confirm the character of behaviours of auxetic plates. Ob-

served differences, for example, smaller values of critical loads obtained for the FEM plate model are important in modelling plates and similar structures.

The main conclusions can be formulated as follows:

- Negative values of Poisson's ratio, which characterise auxetic materials, influence the plate's structural responses through the character of work of the outer plate layers subjected to normal stresses.
- The critical static and dynamic loads increase with the increase of the absolute value of Poisson's ratio of auxetic material of plate facings. The impact of the value of Poisson's ratio is observed, particularly for the examined value $\nu = -0.9$, which is close to the number $\nu = -1$.
- The form of buckling is asymmetric. Therefore, the problem cannot be limited to the axisymmetric one. The proposed approximate analytical and numerical solution, whose fundamentals have been used in calculations related to traditional plates, enables the effective investigation of new plate structures.
- The effect of the auxetic facings does not change the buckling reaction of plates with conventional facings (the results for $\nu = -0.3$ and $\nu = 0.3$).

The presented results show the behaviour of the auxetic three-layered plates on the special layer property expressed by the negative value of Poisson's ratio. In general, it can be observed that plate responses have a structured character and, in a qualitative range, can be predicted. The evaluation of the plate's behaviours can be further conducted, including the complex thermo-mechanical loads for auxetic layered plate structures that are transversely heterogeneous.

References

1. Chen Y.-R., Chen L.-W., Wang C.-C., Axisymmetric dynamic instability of rotating polar orthotropic sandwich annular plates with a constrained damping layer, *Composite Structures*, **73**(3): 290–302, 2006, doi: 10.1016/j.compstruct.2005.01.039.
2. Wang H.-J., Chen L.-W., Axisymmetric dynamic stability of rotating sandwich circular plates, *Journal Vibration and Acoustics*, **126**(3): 407–415, 2004, doi: 10.1115/1.1688765.
3. Alipour M.M., Shariyat M., Analytical zigzag formulation with 3D elasticity corrections for bending and stress analysis of circular/annular composite sandwich plates with auxetic cores, *Composite Structures*, **132**: 175–197, 2015, doi: 10.1016/j.compstruct.2015.05.003.
4. Pham H.C., Pham M.P., Hoang T.T., Duong T.M., Nguyen D.D., Static bending analysis of auxetic plate by FEM and a new third-order shear deformation plate theory, *VNU Journal of Science: Natural Sciences and Technology*, **36**(1), 2020, doi: 10.25073/2588-1140/vnunst.5000.
5. Shariyat M., Alipour M.M., Analytical bending and stress analysis of variable thickness FGM auxetic conical/cylindrical shells with general tractions, *Latin American Journal of Solids and Structures*, **14**(5): 805–843, 2017, doi: 10.1590/1679-78253413.
6. Lim T.-C., Circular auxetic plates, *Journal of Mechanics*, **29**(1): 121–133, 2013, doi: 10.1017/jmech.2012.113.

7. Lim T.-C., Buckling and vibration of circular auxetic plates, *Journal of Engineering of Materials and Technology*, **136**(2): 021007, 2014, doi: 10.1115/1.4026617.
8. Faghfouri S., Rammerstorfer F.G., Buckling of stretched disks – with comparisons and extensions to auxetics, *International Journal of Mechanical Sciences*, **213**: 106876, 2022, doi: 10.1016/j.ijmecsci.2021.106876.
9. Li C., Shen H.-S., Wang H., Nonlinear dynamic response of sandwich plates with functionally graded auxetic 3D lattice core, *Nonlinear Dynamics*, **100**(4): 3235–3252, 2020, doi: 10.1007/s11071-020-05686-4.
10. Tran T.T., Pham Q.H., Nguyen-Thoi T., Tran T.-V., Dynamic analysis of sandwich auxetic honeycomb plates subjected to moving oscillator load on elastic foundation, *Advances in Materials Science and Engineering*, **2020**: Article ID 6309130, 2020, doi: 10.1155/2020/6309130.
11. Behravan Rad A., Static analysis of non-uniform 2D functionally graded auxetic-porous circular plates interacting with the gradient elastic foundations involving friction force, *Aerospace Science and Technology*, **76**: 315–339, 2018, doi: 10.1016/j.ast.2018.01.036.
12. Volmir A.S., *The Nonlinear Dynamic of Plates and Shells* [in Russian: *Nelineinaya Dinamika Plastinok i Obolochek*], Science, Moscow, 1972.
13. Pawlus D., Dynamic stability of three-layered annular plates with wavy forms of buckling, *Acta Mechanica*, **216**(1): 123–138, 2011, doi: 10.1007/s00707-010-0352-3.
14. Pawlus D., Solution to the problem of axisymmetric and asymmetric dynamic instability of three-layered annular plates, *Thin-Walled Structures*, **49**(5): 660–668, 2011, doi: 10.1016/j.tws.2010.09.013.
15. Pawlus D., Dynamic stability of three-layered annular plates with viscoelastic core [in Polish], *Scientific Bulletin of the Technical University of Lodz*, 1075; Technical University of Lodz, Lodz, 2010.
16. Volmir A.S., *Stability of Deformed System* [in Russian: *Ustoichivost Deformiruemykh Sistem*], Science, Moscow, 1967.
17. Wojciech S., Numerical solution of the problem of dynamic stability of annular plates [in Polish: Numeryczne rozwiązanie zagadnienia stateczności dynamicznej płyt pierścieniowych], *Journal of Theoretical and Applied Mechanics*, **17**(2), 247–262, 1979.
18. *ABAQUS/Standard. User's Manual*, Hibbit, Karlsson & Sorensen, Inc., Pawtucket, RI, USA, 1998.
19. Donescu S., Chiroiu V., Munteanu L., On the Young's modulus of a auxetic composite structure, *Mechanics Research Communications*, **36**(3): 294–301, 2009, doi: 10.1016/j.mechrescom.2008.10.006.
20. Pawlus D., Static stability of composite annular plates with auxetic properties, *Materials*, **15**(10): 3579, 2022, doi: 10.3390/ma15103579.

Received December 17, 2022; accepted version May 29, 2023.